Progress In Electromagnetics Research C, Vol. 71, 141–148, 2017

Compact Wide-Beam Circularly Polarized Antenna with Stepped Arc-Shaped Arms for CNSS Application

Can Wang*, Fushun Zhang, Fan Zhang, Yali Yao, and Tian Li

Abstract—A single-feed circularly polarized wide-beam antenna is proposed for Compass Navigation Satellite System (CNSS) application. The antenna consists of four stepped arc-shaped arms, which are applied to generate circularly polarized radiation. To broaden the beamwidth, each arm is split up into two horizontal arc-shaped parts and one vertical part. The proposed antenna is simulated, fabricated and tested. The measured results show that the 10-dB return loss band of the proposed antenna is from 2.37 GHz to 2.65 GHz and the 3-dB axial ratio band from 2.42 GHz to 2.55 GHz, covering the receiving band (2.49175 GHz ± 4.08 MHz) of CNSS. Its 3-dB AR beamwidth is 181° at 2.491 GHz. For the horizontal radiation pattern of the proposed antenna at 5° elevation angle, the RHCP gain is greater than −1.1 dBic, and the out-of-roundness is 1 dB. Additionally, the proposed antenna has a size of $0.37\lambda_0 \times 0.37\lambda_0 \times 0.11\lambda_0$ with respect to 2.491 GHz.

1. INTRODUCTION

Compass Navigation Satellite System (CNSS) or "BeiDou" is one of the popular satellite positioning and navigation systems. Its downlink band is 2.49175 GHz ± 4.08 MHz. For suppressing multipath distortion, reducing polarization mismatch losses and Faraday rotation effects caused by the ionosphere and receiving a better signal from the satellite at any place on the earth, it requires a circularly polarized (CP) antenna with 3-dB AR beamwidth of more than 120° and a relatively high gain at low elevation angle. According to the official performance specifications, the gain of CNSS antennas for 5° elevation angle should be more than −3 dBic, and its out-of-roundness for the horizontal radiation pattern at 5° elevation angle must be less than 3 dB [1].

To broaden the 3-dB AR beamwidth and improve the gain at low elevation angle, much excellent effort has been made in recent years. Quadrifilar helix antenna (QHA) [2–7] is a typical solution to meet circular polarization and wide spatial coverage requirements. However, the gain requirement at low elevation angle is satisfied at the expense of high profile. Some improved crossed dipoles are studied to broaden the beamwidth. Antennas in [8–10] have beamwidths of 180°, 170°, and 160°, respectively. However, these antennas are bulky because they use power divider [8] and metallic cavities [9, 10]. Besides, microstrip antennas with a three-dimensional square ground [11] and four unequal circular patches integrated symmetrically onto corners [12] are proposed, whose 3-dB AR beamwidths are improved up to 113° and 180°, respectively. But height of antenna [11] is more than 0.45 wavelength. Using two pairs of radiators in square contour, 3 dB AR beamwidths of 126° [13] and 175° [14] are obtained, respectively. However, gains in [9–14] at 5° elevation angle are all less than −3 dBic. In order to improve the gain at low elevation angle, some techniques have been put forward in [1, 15–17]. Parasitic ring at the top of traditional microstrip CP antenna is used in [1], and its average gain for 5° elevation angle is about −1.8 dBic. The antennas using vertically loaded elements [15] and a dual-ring cavity [16] are proposed. Their average gains at 5° elevation angle are more than −1 dBic, and the

Received 22 December 2016, Accepted 3 February 2017, Scheduled 17 February 2017
* Corresponding author: Can Wang (wcanxdxd@163.com).
The authors are with the National Key Laboratory of Antennas and Microwave Technology, Xidian University, Xi'an 710071, China.

3 dB AR beamwidth is 180° and 130°, respectively. In [17], pattern diversity is used to radiate circular polarization with the gain of the upper half space more than −1 dBic, but it is fed with two ports.

In this paper, we propose a compact single-feed wide-beam CP antenna. The antenna consists of four stepped arc-shaped arms. Each of the arms is made up of two parts etched on two separated square substrates connected by metallic cylinders, which can improve the average gain for 5° elevation angle up to −0.5 dBic. Circular polarization is achieved over the entire upper hemisphere with the self-phasing method. Moreover, it has a good omnidirectional characteristic for horizontal radiation pattern. In addition, the proposed antenna has a low profile of $0.11\lambda_0$ with respect to 2.491 GHz.

2. ANTENNA STRUCTURE

Figure 1 shows the geometry of the proposed wide-beam CP antenna. The antenna is composed of four arc-shaped radiation arms. Each arm is split up into two horizontal arc-shaped parts and one vertical part. The two horizontal arc-shaped parts are printed on the front or back side of the two separated substrates connected by metallic cylinders. The two separated substrates both have a dimension of $L \times L \times h$, relative permittivity of $\varepsilon_r = 2.65$ and loss tangent of $\tan\theta = 0.02$.

From $+z$ view, the corresponding circle centers for the four arc-shaped arms are $O_1(0, -s)$, $O_2(s, 0)$, $O_3(0, s)$ and $O_4(-s, 0)$, respectively, as shown in Figure 1(a), and their radii R are identical. The printed part of each arm is divided into three arc-shaped steps with widths of W_{m1}, W_{m2}, W_{m3} and angles of θ_{m1}, θ_{m2}, θ_{m3}. As shown in Figure 1(b), the vertical parts between the two separated substrates has a height of H and radius of r. Especially, $W_{m1} = W_4$, $W_{m2} = W_5$, $W_{m3} = W_6$ ($m = 1, 2, 3, 4$), $\theta_{31} = \theta_{11}$, $\theta_{32} = \theta_{12}$, $\theta_{33} = \theta_{13}$, $\theta_{41} = \theta_{21}$, $\theta_{42} = \theta_{22}$, $\theta_{43} = \theta_{23}$, as shown in Figures 1(c) and (d). The printed parts of the stepped arms having angles of θ_{11}, θ_{12} and θ_{13} are located at the front side of the two separated substrates, and those having angles of θ_{21}, θ_{22} and θ_{23} are located at the back side. The total length of each arm is designed to be about 3/4 wavelength in free space at 2.491 GHz. Based on the mechanism given out in Section 3 and through extensive optimizations, the detailed dimensions are obtained and listed in Table 1. In practice, magnetic core is used to balance the current between the coaxial cable and the proposed antenna.

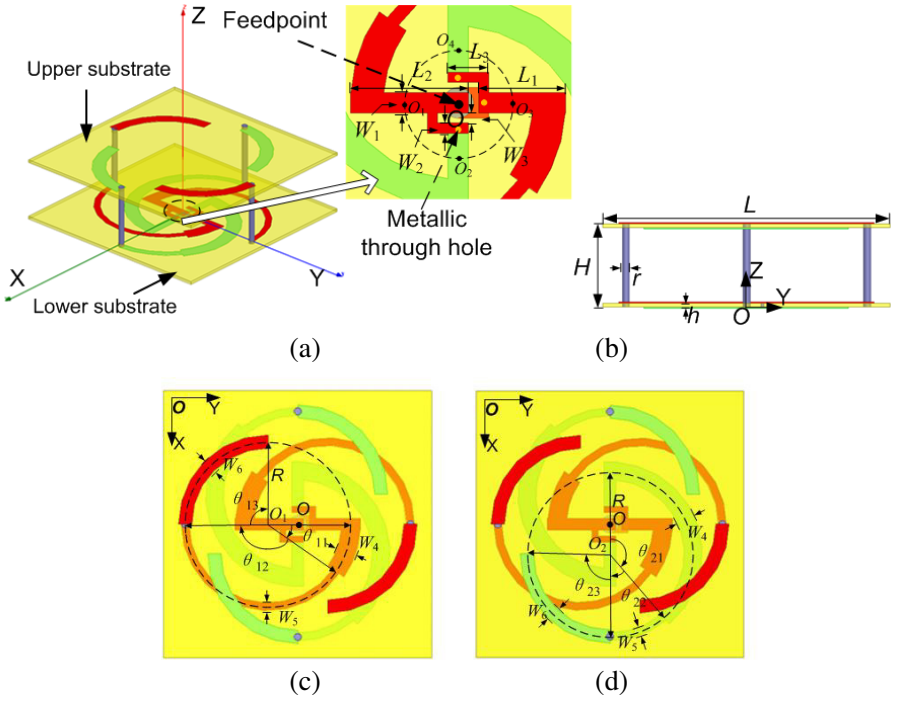

Figure 1. Geometry of the proposed antenna, (a) 3D view, (b) side view, (c) top view with size of red radiation arm, (d) top view with size of green radiation arm.

Table 1. Optimized parameters of the proposed antenna.

parameter	L	L_1	L_2	L_3	W_1	W_2	W_3
Value	45 mm	8.5 mm	11.5 mm	4 mm	2 mm	1 mm	1 mm
parameter	W_4	W_5	W_6	θ_{11}	θ_{12}	θ_{13}	θ_{21}
value	3.2 mm	1.3 mm	2.2 mm	35°	145°	90°	140°
parameter	θ_{22}	θ_{23}	H	r	s	h	R
value	40°	90°	13.2 mm	0.6 mm	5 mm	0.6 mm	18.9 mm

3. MECHANISM OF CIRCULAR POLARIZATION

The mechanism of circular polarization is analyzed in this section. The circular polarization mechanism of the proposed antenna is the same as that of the conventional quadrifilar antenna. In order to achieve CP radiation, it is essential that there are 0°, 90°, 180° and 270° phase differences in the four radiation arms. Figure 2 shows the current distribution on the four stepped arms viewed from the $+z$ direction. It can be found that when the time phase $t = 0°$, the current on arm1 and arm3 is maximum and in the $+y$ direction. When the time phase $t = 90°$, the current on arm2 and arm4 is maximum and in the $-x$ direction. It indicates that after one quarter-period, the current rotates in the right-hand direction by 90° around $+z$ direction, so the 90° phase difference is obtained between arm1 (arm2) and arm4 (arm3). In addition, the 180° phase difference between arm1 (arm4) and arm3 (arm2) is naturally obtained from the inner conductor (connected to arm1 and arm4) and outer conductor (connected to arm2 and arm3) of the coaxial line. Finally, the requirement of phase is satisfied for circular polarization.

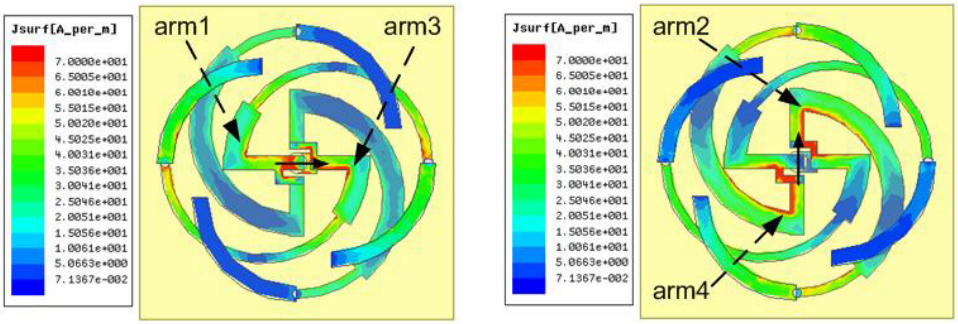

(a) (b)

Figure 2. Current distributions at 2.491 GHz, (a) 0°, (b) 90°.

From the perspective of equivalent circuit, the antenna can be regarded as the parallel connection of the two transmission lines as shown in Figure 3(a). Arm1 and arm3 are equivalent to transmission line B, and arm2 and arm4 are equivalent to transmission line A. The two transmission lines are divided into three steps having the same corresponding characteristic impedances Z_1, Z_2, Z_3 and lengths L_{m1}, L_{m2}, and L_{m3} ($m = 1, 2$), respectively, especially $L_{13} = L_{23}$. $Z_{L_{m2}}$ ($m = 1, 2$) is the load impedance of the second step of the transmission line.

Based on the transmission line theory, the input impedance of the two transmission lines can be calculated as follows ($m = 1, 2$).

$$Z_{in\_m} = Z_1 \frac{\left(Z_2 Z_{L_{m2}} - Z_1 Z_{L_{m2}} \tan\beta L_{m1} \tan\beta L_{m2} + j\left(Z_1 Z_2 \tan\beta L_{m1} + Z_2^2 \tan\beta L_{m2}\right)\right)}{\left(Z_1 Z_2 - Z_2^2 \tan\beta L_{m1} \tan\beta L_{m2} + j\left(Z_2 Z_{L_{m2}} \tan\beta L_{m1} + Z_1 Z_{L_{m2}} \tan\beta L_{m2}\right)\right)} \quad (1)$$

Because characteristic impedances of the three corresponding steps of the two transmission lines are the same and lengths $L_{13} = L_{23}$, the input impedances Z_{in_1} and Z_{in_2} are decided by L_{1n} and L_{2n},

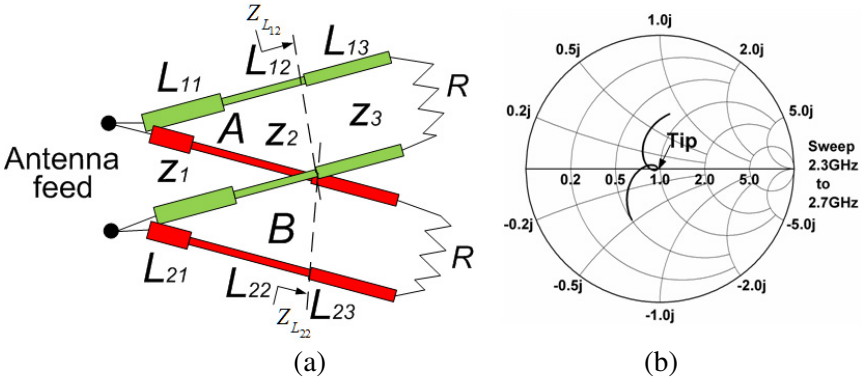

(a) (b)

Figure 3. (a) The equivalent circuit, (b) Smith chart of the proposed antenna.

(n = 1, 2), respectively. In addition, L_{m1} and L_{m2} (m = 1, 2) are corresponding to angles θ_{m1} and θ_{m2} as shown in Figures 1(c) and (d). Then, if θ_{m1} and θ_{m2} are properly tuned, the input impedance of the two pairs of the radiation arms can be adjusted to be inductive and capacitive, respectively. The operating mechanism of the proposed antenna is similar to that of the self-phasing quadrifilar antenna [18]. The Smith chart of the proposed antenna is shown in Figure 3(b). A tip can be found around 2.491 GHz, which indicates that the self-phasing state occurs.

4. PARAMETRIC STUDY

The proposed antenna is simulated and optimized using the ANSYS High Frequency Structure Simulator (HFSS) ver.13 based on the finite element method (FEM). The parameters that are key factor to the design are studied and discussed in this section. When one parameter is varied, all other parameters are kept constant as listed in Table 1.

4.1. Effects of Height H on the Antenna Performance

H is the height of the four metallic cylinders which are the vertical portions of the radiation arms. Figure 4 shows the simulated results with varying H. As H increases from 12.2 mm to 14.2 mm, S_{11} shifts to lower frequencies as shown in Figure 4(a).

In the horizontal direction of the far field of the proposed antenna, the vertical portion of the radiation arms has only E_θ component, and the arc-shaped portion has only E_φ component, which result in good CP radiation at the horizontal plane. Finally, the proposed antenna has a wider 3-dB AR beamwidth and higher gain at the horizontal plane than conventional microstrip antenna. It can

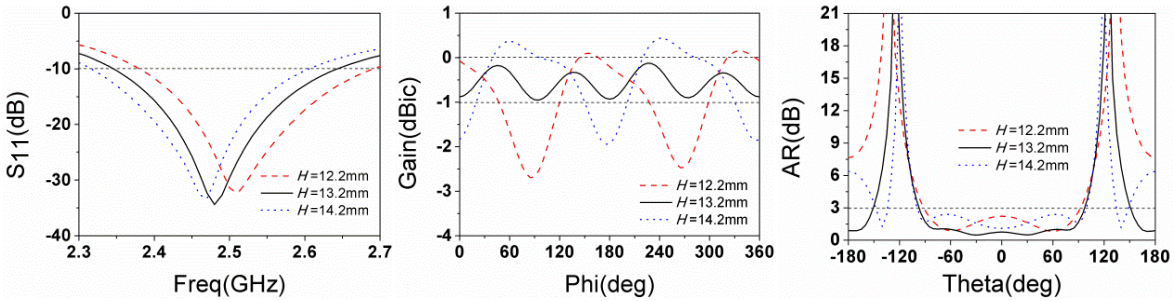

(a) (b) (c)

Figure 4. Simulated results with varying H, (a) S_{11}, (b) gain of XY-plane at $\theta = 85°$, (c) AR at XZ-plane.

be found that when H becomes short, the out-of-roundness of XY-plane at $\theta = 85°$ is deteriorated; AR is worse at $\theta = 90°$; 3-dB AR beamwidth becomes narrow, as shown in Figure 4(b) and Figure 4(c). It is found that 13.2 mm is the best value for H through careful optimization.

4.2. Effects of Angles θ_{11}, θ_{12}, θ_{21}, θ_{22} on the Antenna Performance

According to the mechanism discussion, the performance of the proposed antenna is sensitive to the stepped arms. For the purpose of revealing the effects of the stepped arms on the proposed antenna performance, θ_{11}, θ_{12}, θ_{21} and θ_{22} are studied in this section with the total angle of each arm unchanged and $\theta_{13} = \theta_{23}$.

As can be seen from Figures 5 and 6, when $\theta_{11} = \theta_{21} = 35°$, $\theta_{12} = \theta_{22} = 145°$ or $\theta_{11} = \theta_{21} = 140°$, $\theta_{12} = \theta_{22} = 40°$, the antenna cannot obtain a good performance. This is because the distributions of the currents on the four arms are similar, and 90° phase difference is unable to be obtained. Thereby, it is crucial that θ_{11}/θ_{12} is smaller than θ_{21}/θ_{22} to achieve better right-hand CP radiation toward $+z$ direction, as shown in Figure 5(c) and Figure 6(c). When $\theta_{11} = 10°$, $\theta_{12} = 170°$, $\theta_{21} = 140°$, $\theta_{22} = 40°$ or $\theta_{11} = 35°$, $\theta_{12} = 145°$, $\theta_{21} = 170°$, $\theta_{22} = 10°$, the return loss could be worse, as given in Figure 5(a) and Figure 6(a), so the value of $|\theta_{11}/\theta_{12} - \theta_{21}/\theta_{22}|$ should not be too large.

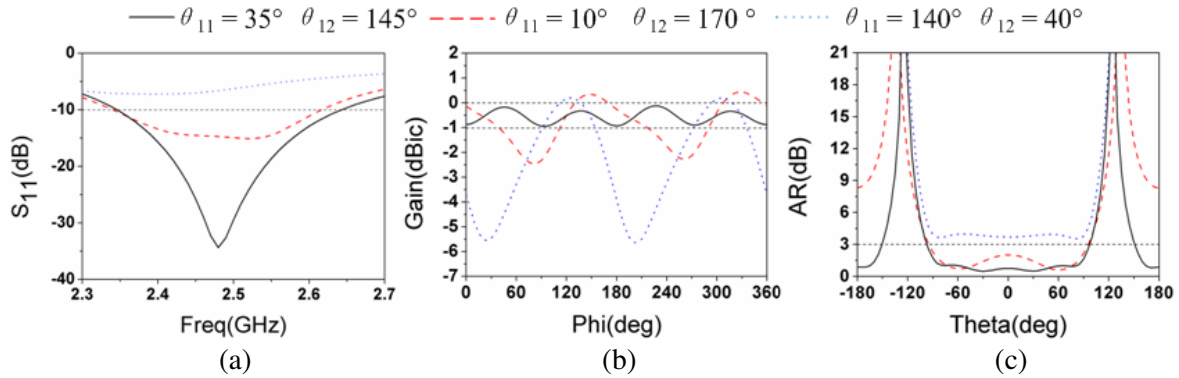

Figure 5. Simulated results with varying θ_{11} and θ_{12}, (a) S_{11}, (b) gain of XY-plane at $\theta = 85°$, (c) AR at XZ-plane.

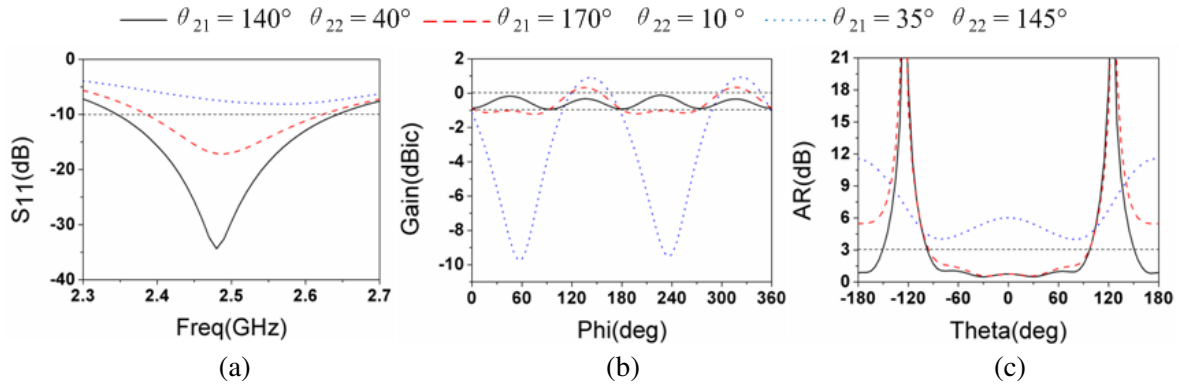

Figure 6. Simulated results with varying θ_{21} and θ_{22}, (a) S_{11}, (b) gain of XY-plane at $\theta = 85°$, (c) AR at XZ-plane.

5. EXPERIMENTAL RESULTS AND COMPARISON

On the basis of the studies in previous sections, the proposed antenna is fabricated and measured successfully to validate the design. Figure 7 shows the prototype of the proposed antenna. The proposed

antenna fed at the center of lower substrate is fabricated with two substrates connected by four metallic cylinders and supported by plastic cylinders.

The measured return loss is given in Figure 8(a). The measured S_{11} shifts to lower frequencies compared with the simulated one, which is mainly due to the fabrication error and imperfect testing environment. It is shown that the proposed antenna has a 10-dB return loss band of 2.37–2.65 GHz. The measured gain at boresight and 3-dB AR bandwidth are shown in Figure 8(b). The measured gain of the boresight at 2.491 GHz is 4.1 dBic, and the measured 3-dB AR band is from 2.42 GHz to 2.55 GHz. Both the measured 10-dB return loss band and 3-dB AR band can cover the receiving band of CNSS. Figure 9(a) shows the measured ARs in the XZ-plane at 2.48 GHz, 2.491 GHz, and 2.5 GHz, respectively. It is shown that the proposed antenna has a 3-dB AR beamwidth of 181° (from −91° to 90°) at 2.491 GHz, which indicates good CP pattern at upper half space. Figure 9(b) shows the measured gain and AR for the horizontal radiation pattern at 5° elevation angle at 2.491 GHz. It is

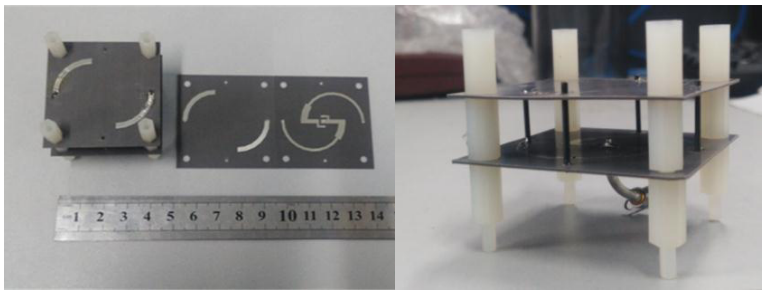

(a) (b)

Figure 7. The prototype of the proposed antenna, (a) top view, (b) side view.

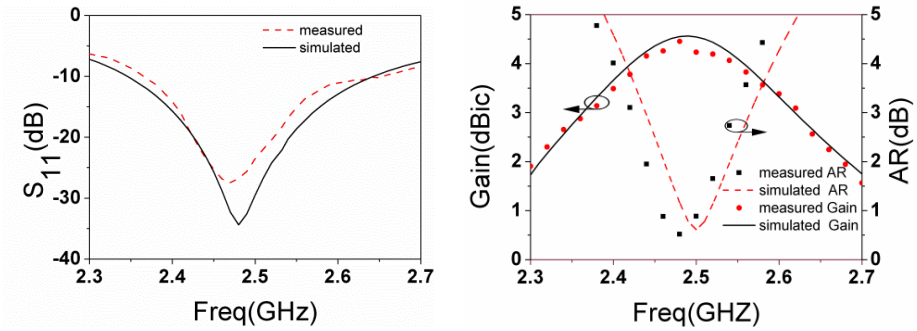

(a) (b)

Figure 8. Measured and simulated results as a function of frequency, (a) S_{11}, (b) gain and AR.

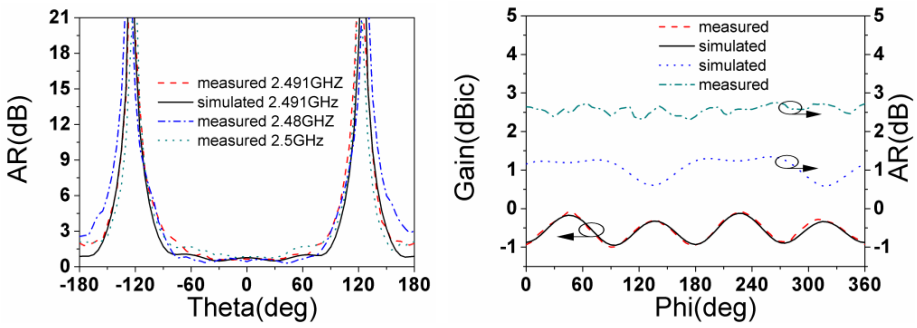

(a) (b)

Figure 9. Measured and simulated results as a function of angle, (a) AR at XZ-plane, (b) gain and AR of XY-plane at $\theta = 85°$ (2.491 GHz).

shown that the gain varies from −1.1 dBic to −0.1 dBic, so the out-of-roundness is about 1 dB. And good circular polarization is obtained at the low elevation angle. The measured and simulated radiation patterns at 2.491 GHz are given in Figure 10. The measured HPBWs are 125° and 123° in the XZ-plane and YZ-plane, respectively. It is shown that the XZ-plane pattern and YZ-plane pattern are quite symmetrical.

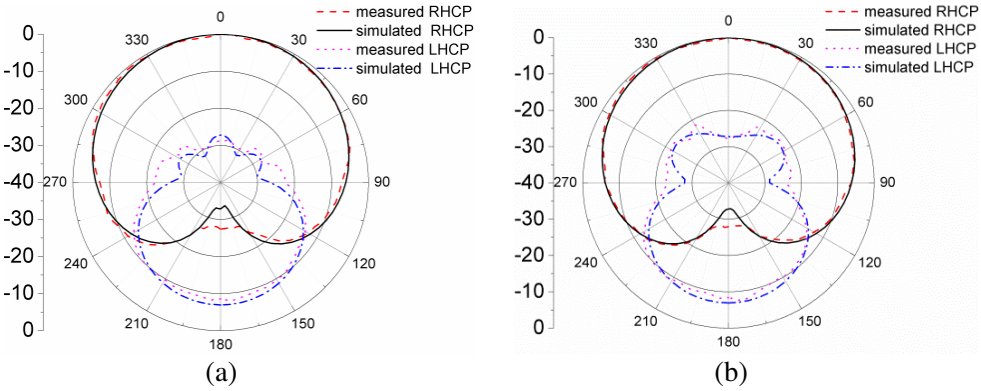

Figure 10. Measured and simulated radiation patterns at 2.491 GHz, (a) XZ-plane, (b) YZ-plane.

Table 2. Comparison between the proposed antenna and the previous antennas.

Reference	Frequency (GHz)	Antenna size (λ_0^3)	3 dB AR beamwidth		Average Gain at 5° elevation angle (dBic)
			XZ-plane	YZ-plane	
[1]	2.492	$\pi \times 0.28^2 \times 0.11$	140°	140°	−1.8
[4]	2.492	$\pi \times 0.265^2 \times 0.4$	150°	150°	0.6
[5]	2.492	$\pi \times 0.2^2 \times 0.44$	110°	110°	−0.9
[11]	2.330	$1.2 \times 1.2 \times 0.45$	113°	113°	−7
[12]	1.575	$0.373 \times 0.373 \times 0.016$	180°	180°	−3.5
[13]	1.575	$0.53 \times 0.53 \times 0.004$	126°	126°	−8
This work	2.491	$0.37 \times 0.37 \times 0.11$	181°	180°	−0.5

As given in Table 2, a comparison is made between the proposed antenna and previous antennas in terms of antenna size, 3-dB AR beamwidth and average gain at 5° elevation angle. The proposed antenna and the antennas in [1, 4, 12, 13] have a 3-dB AR beamwidth of more than 120° at both XZ-plane and YZ-plane. The profiles of the antennas in [12, 13] are lower than that of the proposed antenna, but the average gain of the proposed antenna at 5° elevation angle is −0.5 dBic, which is larger than those of the antennas in [1, 12, 13]. Therefore, the proposed antenna has a wide 3-dB AR beamwidth and relatively high gain at low elevation angle.

6. CONCLUSION

A single-feed widebeam CP antenna with stepped arc-shaped arms is proposed in this paper. The introduction of the stepped radiation arms contributes to good impedance matching and CP radiation property. The proposed antenna is simulated, fabricated and measured. The measured results show that the proposed antenna has a 3-dB AR beamwidth of 181°. For the horizontal radiation pattern of the proposed antenna at 5° elevation angle, the RHCP gain is greater than −1.1 dBic, and the out-of-roundness is 1 dB. At the upper-half space, the proposed antenna can radiate good CP wave with a relatively high gain for low elevation angle. The measured results are in good agreement with the simulated ones. In conclusion, the proposed antenna can be a good candidate for CNSS application.

REFERENCES

1. Pan, Z.-K., W.-X. Lin, and Q.-X. Chu, "Compact wide-beam circularly-polarized microstrip antenna with a parasitic ring for CNSS application," *IEEE Trans. Antennas Propag.*, Vol. 62, No. 5, 2847–2850, 2014.
2. Tranquilla, J. M. and S. R. Best, "A study of the quadrifilar helix antenna for global positioning system (GPS) applications," *IEEE Trans. Antennas Propag.*, Vol. 38, No. 10, 1545–1550, 1990.
3. Caillet, M., M. Clenet, A. Sharaiha, and Y. M. M. Antar, "A broadband folded printed quadrifilar helical antenna employing a novel compact planar feeding circuit," *IEEE Trans. Antennas Propag.*, Vol. 58, No. 7, 2203–2209, 2010.
4. Lin, W.-X. and Q.-X. Chu, "Wide beamwidth quadifilar helix antenna with cross dipoles," *Progress In Electromagnetics Research C*, Vol. 40, 229–242, 2013.
5. Chu, Q.-X., W. Lin, W.-X. Lin, and Z.-K. Pan, "Assembled dual-band broadband quadrifilar helix antennas with compact power divider networks for CNSS application," *IEEE Trans. Antennas Propag.*, Vol. 61, No. 2, 516–523, 2013.
6. Hebib, S., N. J. G. Fonseca, P. A. Faye, and H. Aubert, "Compact printed quadrifilar helical antenna with shaped pattern and high cross polarization discrimination," *IEEE Antennas Wireless Propag. Lett.*, Vol. 10, 635–638, 2011.
7. Louvigne, J. C. and A. Sharaiha, "Broadband tapered printed quadrifilar helical antenna," *Electron. Lett.*, Vol. 37, 932–933, 2001.
8. Sun, L., B.-H. Sun, H. Wu, J. Yuan, and W. Tang, "Broadband, wide beam circularly polarized antenna with a novel matching structure for satellite communications," *Progress In Electromagnetics Research C*, Vol. 58, 159–166, 2015.
9. Ta, S. X. and I. Park, "Crossed dipole loaded with magneto-electric dipole for wideband and wide-beam circularly polarized radiation," *IEEE Antennas Wireless Propag. Lett.*, Vol. 14, 358–361, 2015.
10. Ta, S. X., H. Choo, I. Park, and R. W. Ziolkowsk, "Multi-band, wide-beam, circularly polarized, crossed, asymmetrically barbed dipole antennas for GPS applications," *IEEE Trans. Antennas Propag.*, Vol. 61, No. 11, 5771–5775, 2013.
11. Tang, C. L., J. Y. Chiou, and K. L. Wong, "Beamwidth enhancement of a CP microstrip antenna mounted on a three-dimensional ground structure," *Microw. Opt. Technol. Lett.*, Vol. 32, No. 2, 149–153, 2002.
12. Nasimuddin, Y. S. Anjani, and A. Alphones, "A wide-beam CP asymmetric-microstrip antenna," *IEEE Tran. Antennas Propag.*, Vol. 63, No. 8, 3764–3768, 2015.
13. Luo, Y., Q.-X. Chu, and L. Zhu, "A low-profile wide-beamwidth circularly-polarized antenna via two pairs of parallel dipoles in a square contour," *IEEE Trans. Antennas Propag.*, Vol. 63, No. 3, 931–936, 2015.
14. Park, B.-C. and J.-H. Lee, "Compact circularly polarized antenna with wide 3-dB axial-ratio beamwidth," *IEEE Antennas Wireless Propag. Lett.*, Vol. 15, 410–413, 2016.
15. Choi, E.-C., J. W. Lee, and T.-K. Lee, "Modified S-band satellite antenna with Iso flux pattern and circularly polarized wide beamwidth," *IEEE Antennas Wireless Propag. Lett.*, Vol. 12, 1319–1322, 2013.
16. Zuo, S.-L., L. Yang, and Z.-Y. Zhan, "Dual-band CP antenna with a dual-ring cavity for enhanced beamwidth," *IEEE Antennas Wireless Propag. Lett.*, Vol. 14, 867–870, 2015.
17. Deng, C., Y. Li, Z. Zhang, and Z. Feng, "A CP pattern diversity antenna for hemispherical coverage," *IEEE Trans. Antennas Propag.*, Vol. 62, No. 10, 5365–5369, 2015.
18. Wang, Y.-S. and S.-J. Chung, "A miniature quadrifilar helix antenna for global positioning satellite reception," *IEEE Trans. Antennas Propag.*, Vol. 57, No. 12, 3746–3751, 2009.